

AEROMAGNETIC SURVEY OF PORTUGAL (Southern panel)

MIRANDA, J. M. ⁽¹⁾, GALDEANO, A. ⁽²⁾ and MENDES-VICTOR, L. A. ⁽¹⁾

⁽¹⁾ Centro de Geofísica da Universidade de Lisboa
R. Escola Politécnica 58, 1200 Lisboa, Portugal

⁽²⁾ Institut de Physique du Globe de Paris
Tour 2425, 4 Place Jussieu, Paris, 75004, France

(Received 13 July 1987)

ABSTRACT—The Aeromagnetic Survey of Portugal here presented makes possible a high precision mapping of the magnetic anomalies due to crustal heterogeneities. The separation of the measured field into a deep, or normal, part and a shallow one, is achieved by the IGRF80 model. The final magnetic anomalies show a remarkable correlation with the major regional features and the main geological structures.

Data presented here concern only the southern panel of the survey. Flight operations were made in 1978.

1 – INTRODUCTION

The Instituto Nacional de Meteorologia e Geofísica (INMG), in collaboration with the Centro de Geofísica da Universidade de Lisboa (CGUL), planned and executed the Aeromagnetic Survey of Portugal. Their purposes were the accurate mapping of the geomagnetic elements over Portugal and the identification of the magnetic signature of the main structural features in the territory.

Flight operations were carried out by the geophysical team of the Portuguese Air Force with a Geometrics G803 proton precession magnetometer, and took place in the years of 1978 (southern pannel) and 1981 (northern pannel).

Magnetic base stations, also equipped with proton magnetometers were maintained by the INMG in Beja, Tomar and Vila Real in order to provide efficient time reduction of measurements.

Final control of secular variation was achieved by comparison with Magnetic Observatory of Coimbra University.

Data processing took place in the INMG, the CGUL and the Institut de Physique du Globe de Paris, in the framework of the collaboration between the three institutions.

The aim of this work is to present the technical characteristics of the survey with particular emphasis on the main options taken by the authors in all different stages of data processing.

The processing of each panel originated different problems particularly because there is a 3 year time gap between them and also because some differences did exist between field operations methodology for each pannel. So, we decided to discuss and present first the southern pannel, together with its total intensity map for the 1979.0 epoch and its associated anomalies. In a later paper we shall present the northern panel and the final geomagnetic maps.

2 – GENERAL CHARACTERISTICS OF THE AEROMAGNETIC SURVEY

The initial planning of the survey divided the portuguese territory in two panels (here named «southern panel» and «northern panel»). The flight line directions follow the magnetic meridians, 10 Km apart, and numbered from 1 (at west) to 34 (east).

Every 40 Km a tie-line was flown, perpendicularly to the flight lines and numbered from 37 (at the north) to 51 (at the south). Fig. 1 shows the general planning scheme.

The measurement of the geomagnetic field was made with a proton procession magnetometer operating with 1 sec sampling rate, corresponding to near 70 m spacing over the terrain.

The mean flight height was 10 000 feet (approximately 3 000 m) and was controlled by a barometric altimeter.

The horizontal position of the measure points was calculated from aerial photographs, taken every 10 seconds and synchronized with the magnetometer.

A total of 34 flight hours took place, corresponding to approximately 6 700 Km of geomagnetic profiles used for the processing.

From all the lines executed by the Air Force the only ones which were discarded were those aborted during operation and the tie-line 51, because its spatial restitution was considered not reliable.

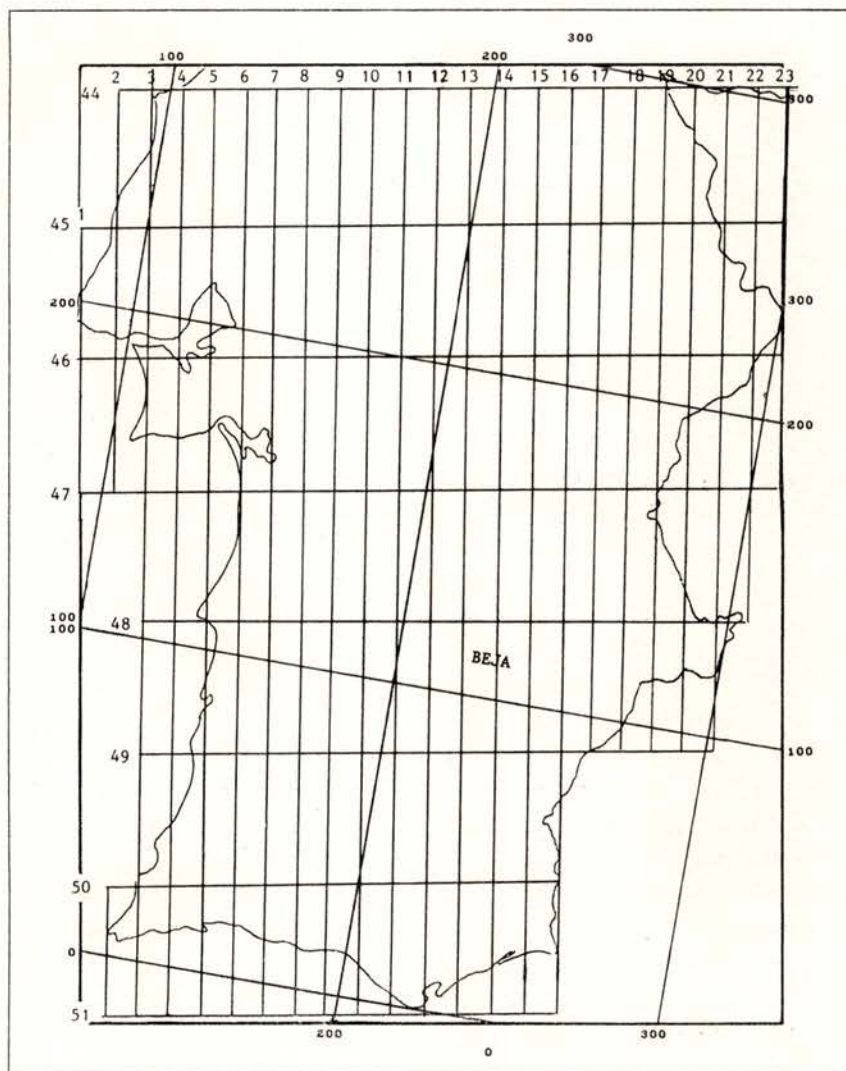


Fig. 1 — Planning of the L. A. P. C. The tie-line 45 divides the northern from the southern panel. The reference station for the southern panel was located in Beja.

3 — SYNTHESIS OF MAIN PROCESSING STEPS

One tenth of the total amount of the photographs executed by the aircraft equipment was geometrically restituted after identification of the sharp features on 1:25000 topographic maps.

The coordinates of the geometrical centres of the photos were sampled and then plotted for validation.

Above the sea, in the areas important to assure a clear definition of the geomagnetic field a careful extrapolation was made based upon the stability of the aircraft movement.

The coordinates of all the measurement points were then calculated by interpolation with cubic splines.

3.1 — *Processing of magnetometer records*

The magnetic tape content, recorded by the plane equipment, includes: (i) code designation of flight line, (ii) sequential numbering of the measurement, (iii) magnetic field's intensity (nT), (iv) day, (v) measurement time with 1 sec precision, and (vi) barometric altitude. Besides this relevant information, other fields were also recorded but we will not consider them in our work.

All the files were filtered with a symmetrical 11 point cosinusoidal, filter and then sampled at 1/10 of the original measurement points. The mean spacing between field values retained is approximately 700 m. This value, when compared with the mean flight height (3 000 m) assures the retention of all relevant magnetic information. The sampling points were also chosen so that they correspond to the photographs really identified.

The filtered field values and geographical coordinates of each measurement point were added into the magnetic tape records.

3.2 — *Reduction stations processing*

The time reduction of field data was essentially based upon the instantaneous comparison between field measures and the reduction station. So, we must be able to know the (annual) mean

field values for each reduction station and we must also be sure that the daily geomagnetic variation is homogeneous for all the panel covered by each station.

The determination of the geomagnetic annual mean field for the reduction station is usually accomplished by the comparison with a permanent magnetic observatory, from which mean values are already known. This is done by the determination of a mean value for the difference between daily magnetic field values at both stations. The difference can also be calculated from measurements at very quiet hours.

Unfortunately, the Beja reduction station was not in operation during the night and so we needed to establish an alternative method for an effective calculation of its mean annual field.

The analogic records for the Beja and Coimbra stations were digitized and sampled with a 100 sec constant step. Then we made the assumption that, for each day d , the time variation at both stations should be related by an expression of the form:

$$B = F * C$$

where B and C have the following components:

$$b_i = \bar{T}_B^d - T_B(t_i) \quad c_i = \bar{T}_C^d - T_C(t_i)$$

The filter F can be calculated in a least squares (LS) sense ($\|B - F * C\| = \min$). However, while \bar{T}_C^d is a known value, \bar{T}_B^d is not and, in this step, is our true unknown.

The calculation process starts with a first guess for \bar{T}_B^d (determined from the true measurement records). This allows a first choice for the filter coefficients f_i from the LS procedure

$$\sum_{m=1}^{NTF} f_m \left[\sum_{n=1}^{NP} c_{n-m+NTF} c_{n-q+NTF} \right] = \sum_{n=1}^{NP} (c_n b_{n-q+NTF})$$

($q = 1, \dots, NTF$)

where NTF and NP are, respectively, the dimensions of the filter and the real data segment.

Then, we can «reconstruct» Beja values from Coimbra measurements and so we will get another guess for \bar{T}_B ; the process is then repeated until we can verify a convergence on \bar{T}_B^d values.

The typical results obtained for the prediction error DF are shown in Fig. 2. We were able to find convergence for every day of the survey.

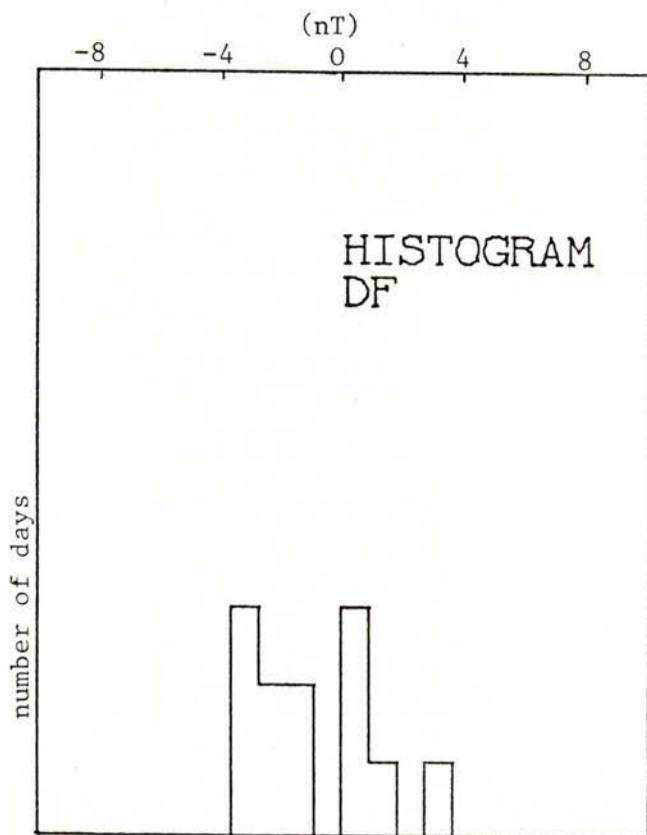


Fig. 2 — Differences between the true daily mean for Coimbra Observatory and the predicted Beja station values.

After applying this methodology to all surveying days we concluded that for all values of d , the differences between daily mean values at Coimbra and Beja are all included in the interval

$$\bar{T}_C^d - \bar{T}_B^d = (790 \pm 4) \text{ nT}$$

The estimated daily differences distribution is shown in Fig. 3.

Coimbra mean annual value for 1979.0 epoch is 44094 nT.
Thus we can deduce the mean value for the Beja station:

$$\bar{T}_{B, 1979.0} = 43305 \text{ nT}$$

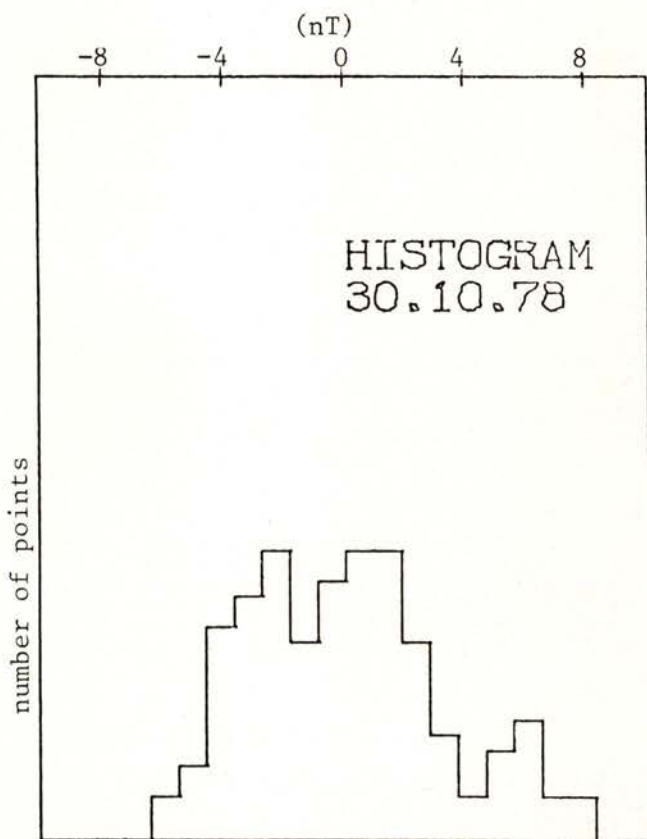


Fig. 3 — Histogram of the prediction error for a typical day
(30 Oct. 1978).

Time reduction of the geomagnetic field measurements is then easily determined from the differences ($\bar{T}_B(t) - 43305 \text{ nT}$) and applied to all field records.

3.3 — *Flight line levelling*

The effectiveness of time and spatial data reduction is essentially verified by the cross errors between flight lines and tie-lines.

Such errors are mainly related to (i) the conductivity anomalies usually due to geological discontinuities, (ii) localization errors, and (iii) inherent inaccuracy of barometric determination of altitude.

The first source of errors affects both flight and tie-lines but the other two are strongly correlated to the horizontal and vertical gradients of the field. The tie-lines must be flown in geomagnetic quiet days and some of them were repeated.

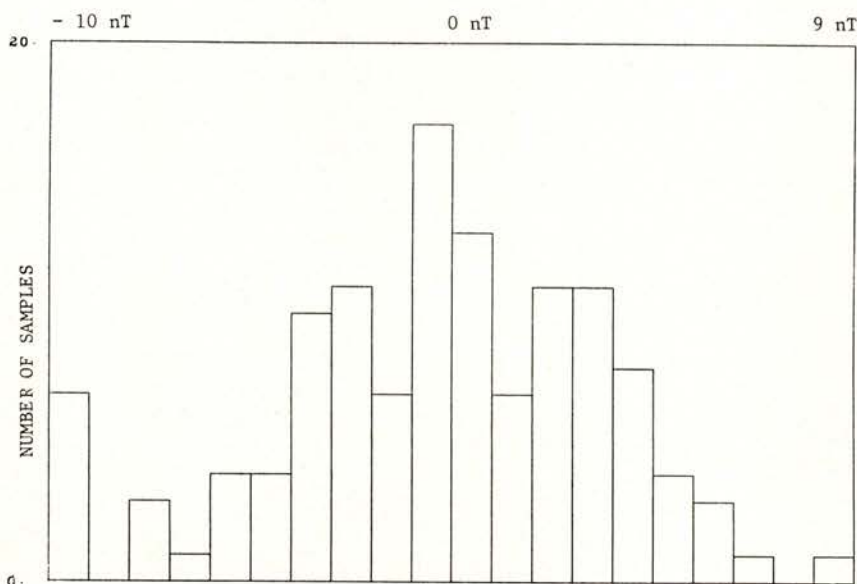


Fig. 4 — Cross error distribution (nT). All flight lines were forced to have null mean cross errors.

The methodology followed in the detection and elimination of cross errors included the following steps: (i) automatic determination of the coordinates of the cross point between each flight

line and all tie-lines, (ii) linear interpolation between the four relevant points for the determination of the error «tie-line minus flight line», (iii) constant correction of each tie-line from the mean cross error with all the flight lines, (iv) final correction of each flight line supposing that the error could be expressed by a cubic spline.

In Fig. 4 we show the histogram of cross errors for the southern panel. A small quantity of high values is related to high horizontal gradient both in the geomagnetic field and the topography or to very particular radio-electrical phenomena that cause a phase lock condition in the magnetometer. In low gradient areas the errors are always small.

3.4 — *Flight line regularization*

The spatial distribution of data points does not match with the previously planned grid and corresponds to equally time sequences rather than to spatial ones because the speed of the aircraft does change during the flight. It is then necessary to perform the interpolation of these field values into a regular grid, that will be the basis of the subsequent processing steps.

The methodology developed by the second author (unpublished) is particularly adapted to aeromagnetic surveys, where data collection is made along profiles. It is divided in the following steps:

- (i) elimination of the spikes (if any) over the profile. This filtering is achieved by fitting smoothing splines [1] to the field data. The measure of the global fitting error is then minimized:

$$\sum_{i=1}^N \left[\frac{F(x(i)) - y(i)}{dy(i)} \right]^2 < S$$

and so, changes in the values of S and the individual weights $dy(i)$ are then related to the smoothing effect, allowing the control for every situation.

- (ii) determination of the optimal location of the regular grid that approximates, in the LS sense, all the coordinates of the data points. This location is mainly characterized

by the coordinates of its east azimuth and the spacing between profiles. The gridded values are then represented by a matrix where the columns correspond to the flight lines.

- (iii) projection of the true field data onto the regular grid, first in the direction of the flight lines and afterwards in the direction of the tie-lines. This projection is made with smoothing splines or by Akima splines [2] according to the smoothing effect needed.

The results obtained in the L. A. P. C. are presented in Figs. 5 and 6. We can assume that the filtering level imposed to the aeromagnetic data is very low. Only a small number of points were significantly changed. On the other hand, Fig. 6 shows that only the flight lines 1 and 2 are particularly far from the calculated grid.

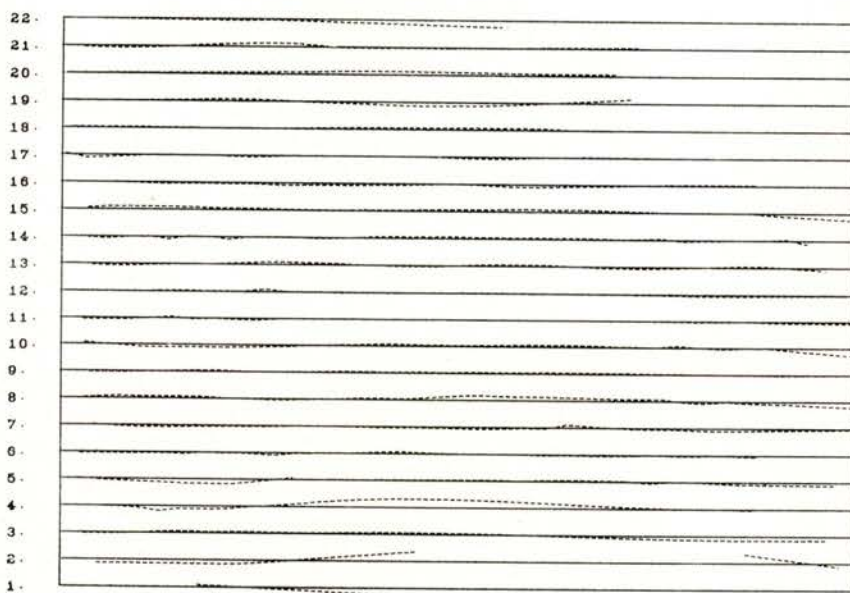


Fig. 5 — Comparison between the true measurement points and grid location.

The final spacing between profiles is 10 Km (the LS value was 10.014 Km) and the east azimuth — 9.8 degrees.

The projection of the flight lines over the regular grid produced a matrix with dimension (304,23) corresponding to a 10 Km spacing between profiles and a 1 Km spacing along each one.

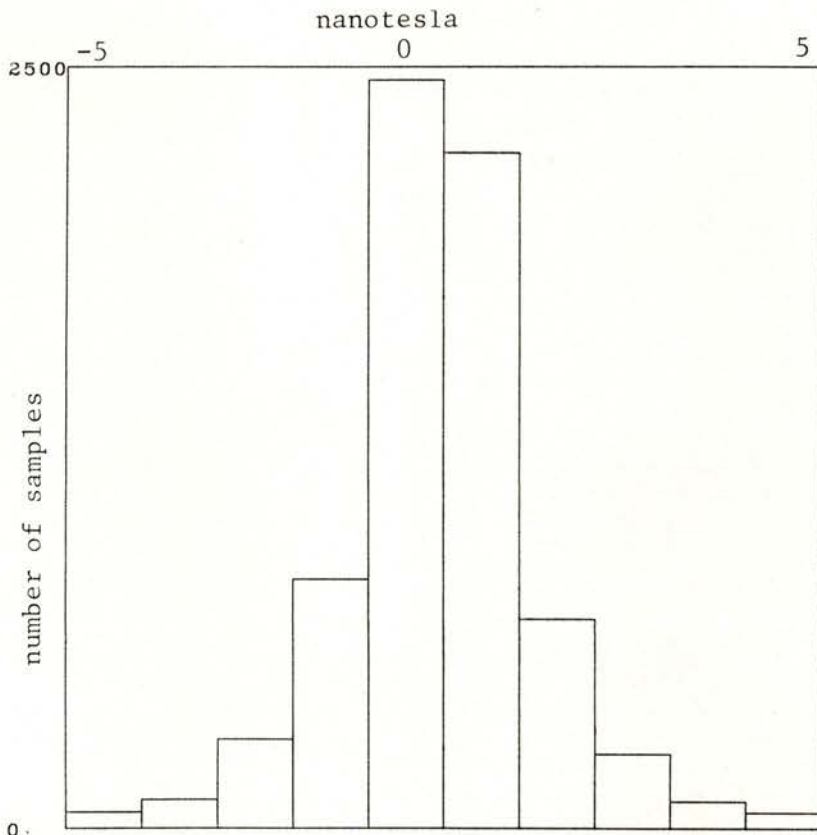


Fig. 6 — Differences between data points before and after smoothing.

Being aware that the spacing between processed data points was approximately 700 m, the 1 Km spacing between retained values assures the fiability of the final representation of the field.

3.5 — *Magnetic field mapping*

The mapping of the geomagnetic field over the horizontal plane is possible if we can assume a spatial representation that is compatible with field data along the measurement profiles.

The basic assumption made was that the magnetic field could be well represented by two dimensional cubic splines [2] fitting the gridded data. This method was proved to be satisfactory to map the field in several aeromagnetic surveys [3].

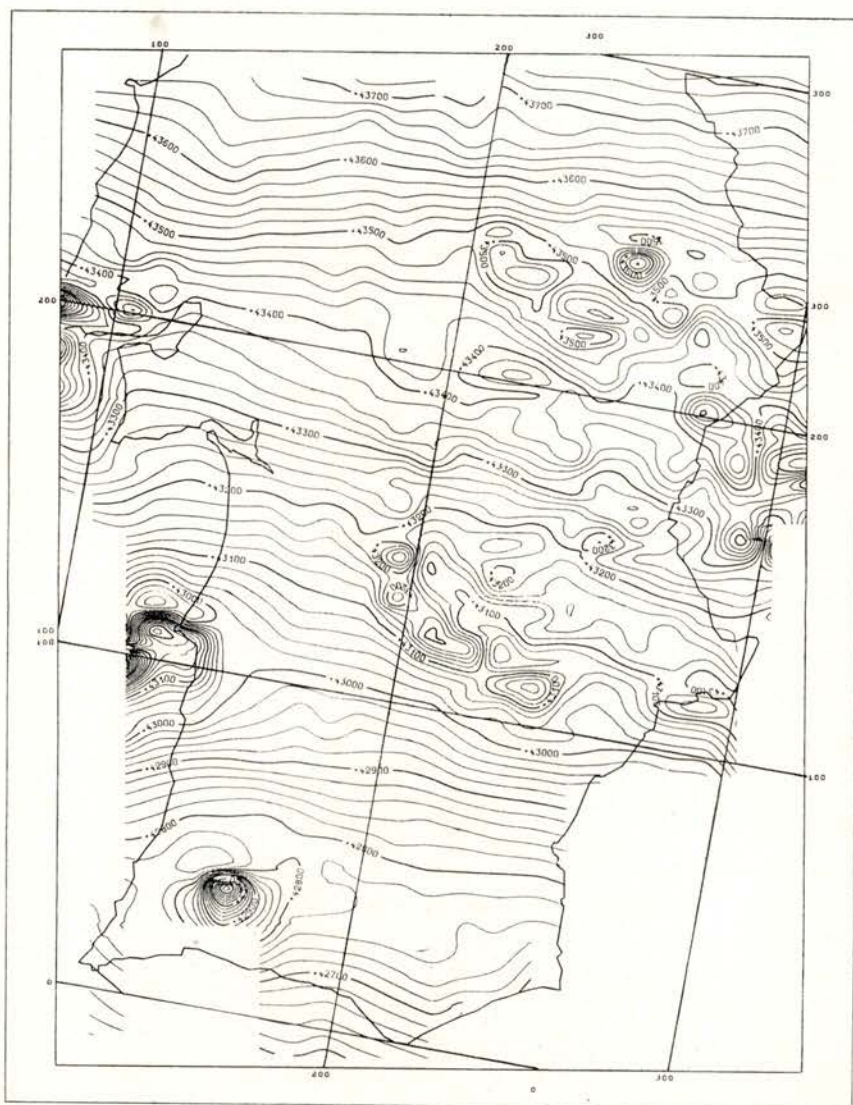


Fig. 7 — Total field map for southern Portugal. Epoch: 1979.0; altitude: 3000 m; equidistance between isovalues: 20 nT.

The aeromagnetic map of southern Portugal for the 1979.0 epoch and the 3000 m altitude is shown in Fig. 7.

4 — NORMAL AND ANOMALOUS COMPONENTS OF THE MAGNETIC FIELD

4.1 — *Polynomial representations*

The total field aeromagnetic map shows a sharp separation between two regions of very different magnetic signatures. The first one corresponds to the Ossa Morena Zone (OMZ) easily identified by the high value of the horizontal gradient, showing an almost perfect delineation of its known geological limits at south, and partially, at west (cf. Ribeiro et al. [4]). The second one corresponds to the South Portuguese Zone (SPZ), where the horizontal gradient is smaller and we can identify three major magnetic anomalies: Monchique, Sines and Sintra, almost aligned, the last two being only partially included in the survey area.

The separation of the measured field into a normal component that must retain the contribution of the deep sources located in the core of the earth, and an anomalous component related to the lateral inhomogeneities of the crust, is strongly constrained by the dimension of the survey area.

We are then in a situation where it is necessary to determine on one hand if it is possible to calculate a polynomial expression for the main field, as is usually done (Le Mouel [5]; Galdeano [3]) and, on the other hand, if the existing global geomagnetic reference fields can successively represent the main field.

The calculation of a polynomial expression for the main field:

$$F^N(x_i; y_i) = \sum_{j=0}^m \sum_{k=0}^n a_{jk} P_j(x_i) P_k(y_i)$$

can be suitably made with orthogonal polynomials (Le Mouel [5]; Mendes-Victor [6]). Their major advantage relies in the fact that, its coefficients being mutually independent, it is easy to divide

a method for estimating the «best» approximation degree, calculated only from the real data.

The determination of the polynomials was done with the recursion formulae given by Berezin and Zhidkov [7]. The corresponding coefficients were calculated for the gridded data by Grant's method [8]. The measure of the fit of the polynomial expansion is given by the behaviour of the residuals:

$$z_{pq}^2 = a_{pq} \| P_p(x) \| \cdot \| P_q(y) \|$$

because they are a measure of the individual contribution to the norm from each polynomial.

—	1923927	1725311	17019	134882	15121	116010	1134	9337
56386115	213299	2345143	65856	140704	60077	298663	41616	
487012	189796	54239	24960	65172	6604	106910	17272	
137044	7447	2290	39821	30872	27952	30719		
8381	20330	41230	2263	20106	3980	23517		
1118	18009	13910	187	47	57478			
12420	18398	20178	11369	27901	3750			
608	6635	106	1425	578				
33134	11129	9652	11007	7409				
10766	707	1154	3659					
55393	21952	648	556					
914	255	61						
20095	8457	82						
326	587							
139	424							
950								
1205								

Fig. 8 — Value of the residuals z_{pq}^2 for the lower order polynomials of the expansion of the total field.

The values of z_{pq}^2 are partially listed in Fig. 8. We can conclude that there is no sharp discontinuity (mainly in the EW direction) as detected in other aeromagnetic surveys, probably because its lateral extension, when compared to the dimensions

of the major magnetic structures, gives rise to the existence of medium range terms in the polynomial expansion that emphasize the magnitude of the EW transition in the total field map.

These results lead to the conclusion that a planar expression for the normal field could be the most suitable, being the least sensitive to regional features. The explicit determination of the coefficients was done with all the original data, by a robust LS procedure. Its values are:

$$F^N(x, y) = 43758.7 - (x - 200000) \times 0.122432734 \times 10^{-3} + \\ (y - 300000) \times 3.7333213882 \times 10^{-3} \text{ nT}$$

where $(x - 200000)$ and $(y - 300000)$ represent the value (in meters) of the national Hayford Gauss coordinates referred to the Cartographical Central point of Portugal. The choice of the origin of the planar model coordinates is the most adequate because it will be the origin for the polynomial expansion of the normal field in the north.

4.3 — *Comparison between the IGRF80 model and the planar expression for the main field*

The chosen model for the International Geomagnetic Reference Field was the IGRF80 [9] that corresponds to an expression of the earth's main magnetic field in Schmidt spherical harmonics of degree and order 10, whose coefficients were deduced from Observatory and Satellite data.

The corresponding map for Portugal (epoch: 1979.0, height 3000 m) is presented in Fig. 9. It is very similar to that obtained from the planar model both in the values of the field and its gradient.

However, a closer analysis of both reference fields allows the identification of a «non-planar» component in the IGRF80 that can be easily shown by the corresponding differences map (Fig. 10).

The morphology of the IGRF can be well fitted locally by a second degree polynomial. It might be thought that a parabolic fit of survey data would give a better expression for the normal

field. However (see Fig. 11) this would, once more, be severely influenced by the lateral limitations of the survey.

Being aware that the IGRF80 gives the possibility of combining the local fit of the data with the constraints introduced from the

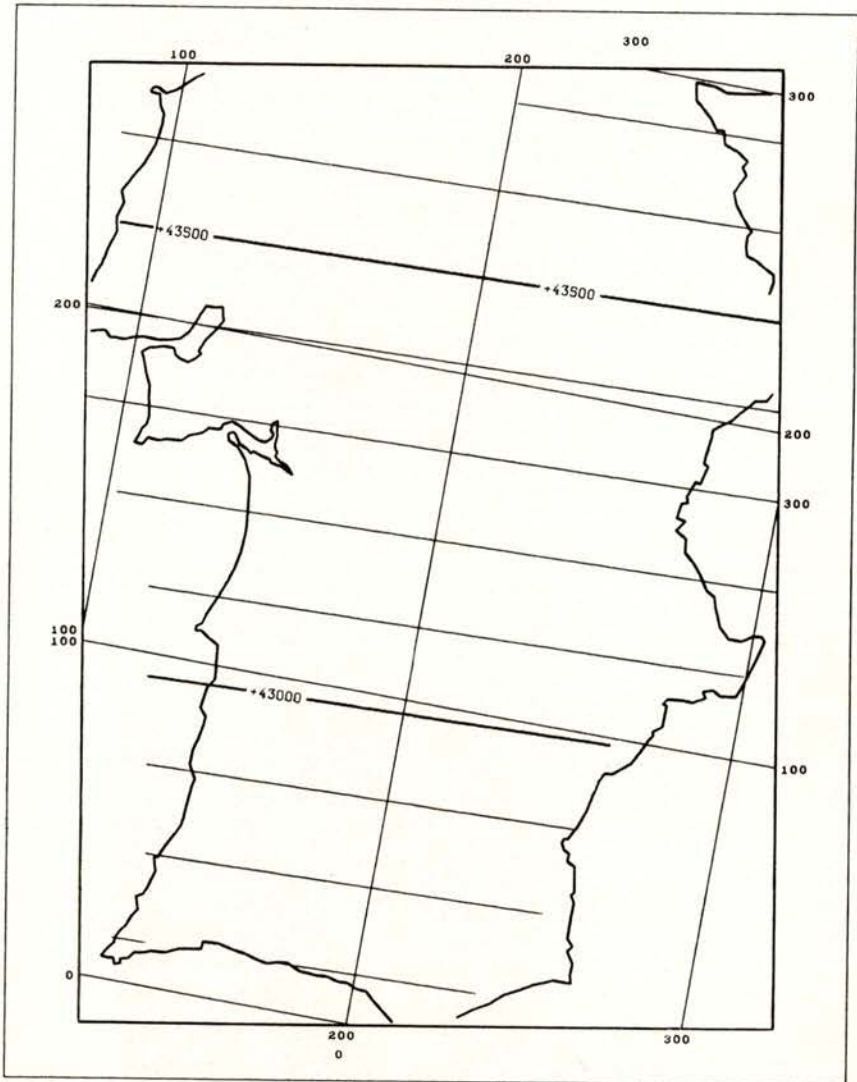


Fig. 9 — Normal fields deduced from IGRF80 (a) and planar approximation of the survey data (b). Isovalues are plotted every 100 nT.

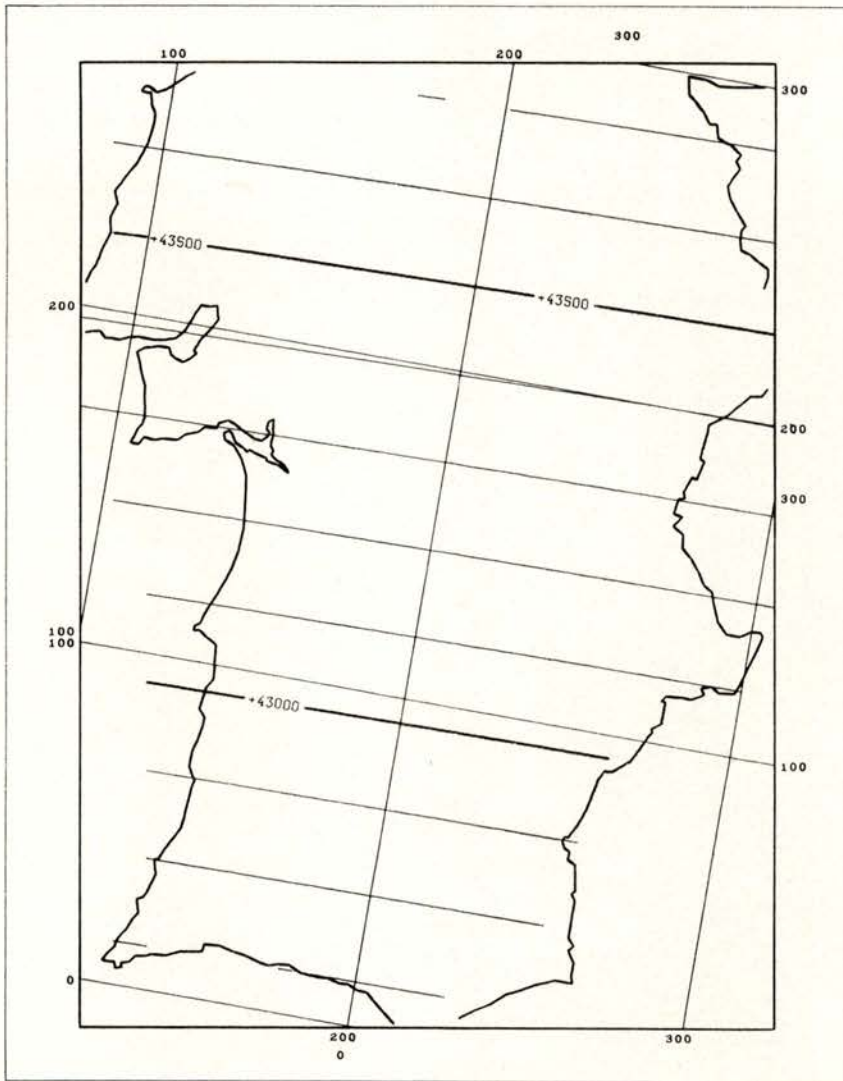


Fig. 9 (b)

analysis of the global main field, it is better to use the IGRF80 to define the normal field. The only slight change that must be done in this representation is to subtract 17 nT from IGRF value, in order to achieve a null mean over the area covered by the survey.

The map of the total field anomalies is presented in Fig. 12. The observations made concerning the total field map are now more obvious. The boundaries of the OMZ and SPZ are magnetically sharp, the SPZ being mainly characterized by small/medium range wavelength magnetic anomalies, and the OMZ being an anomalous

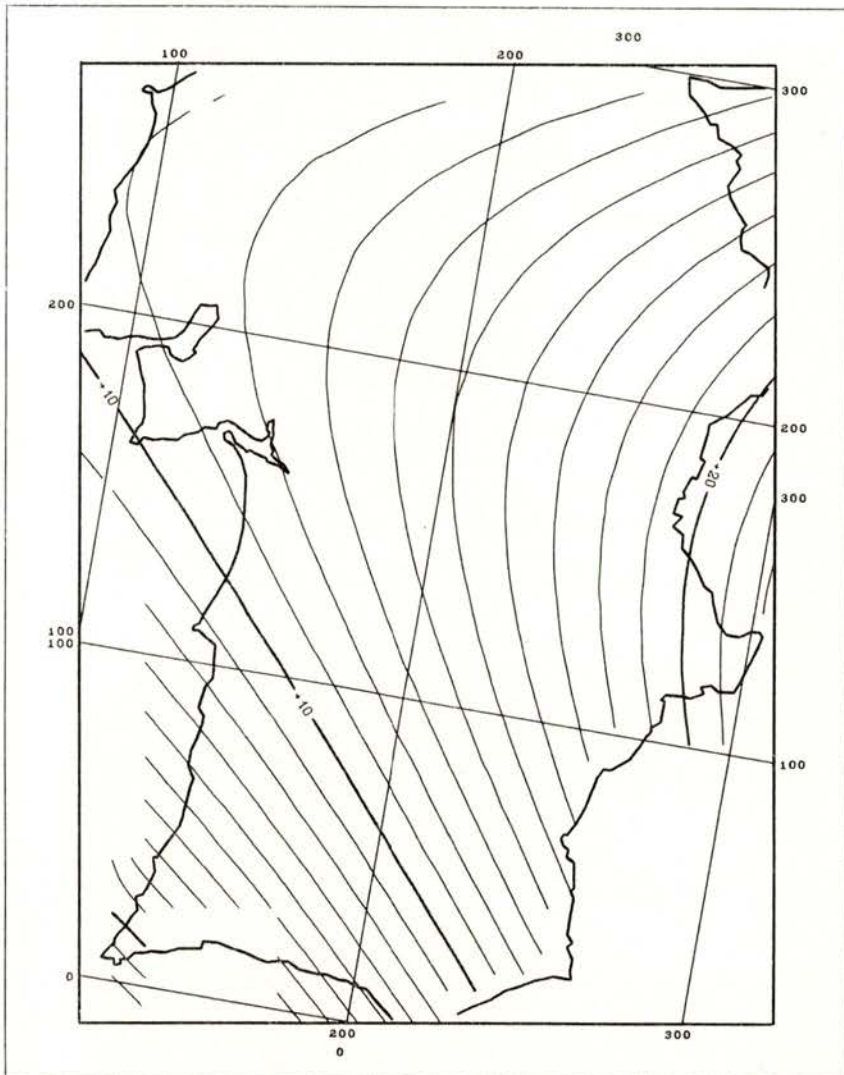


Fig. 10 — Differences (nT) between IGRF80 and the planar model.

area, with various small wavelength anomalies, surely related to shallow magnetic structures.

The morphology of the anomalous total field, and in particular the location of the zero anomaly level seems to confirm the validity of the procedure adopted.

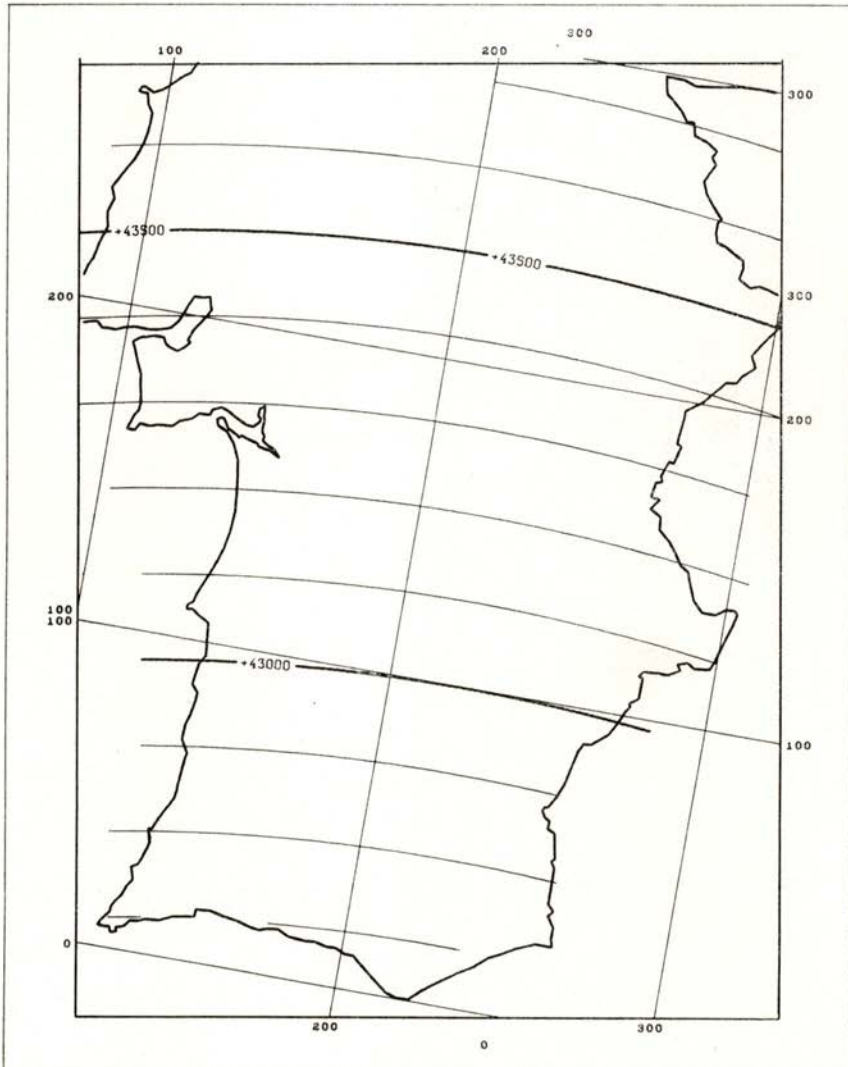


Fig. 11 — Parabolic fitting of survey data. Distance between isolines: 100 nT.

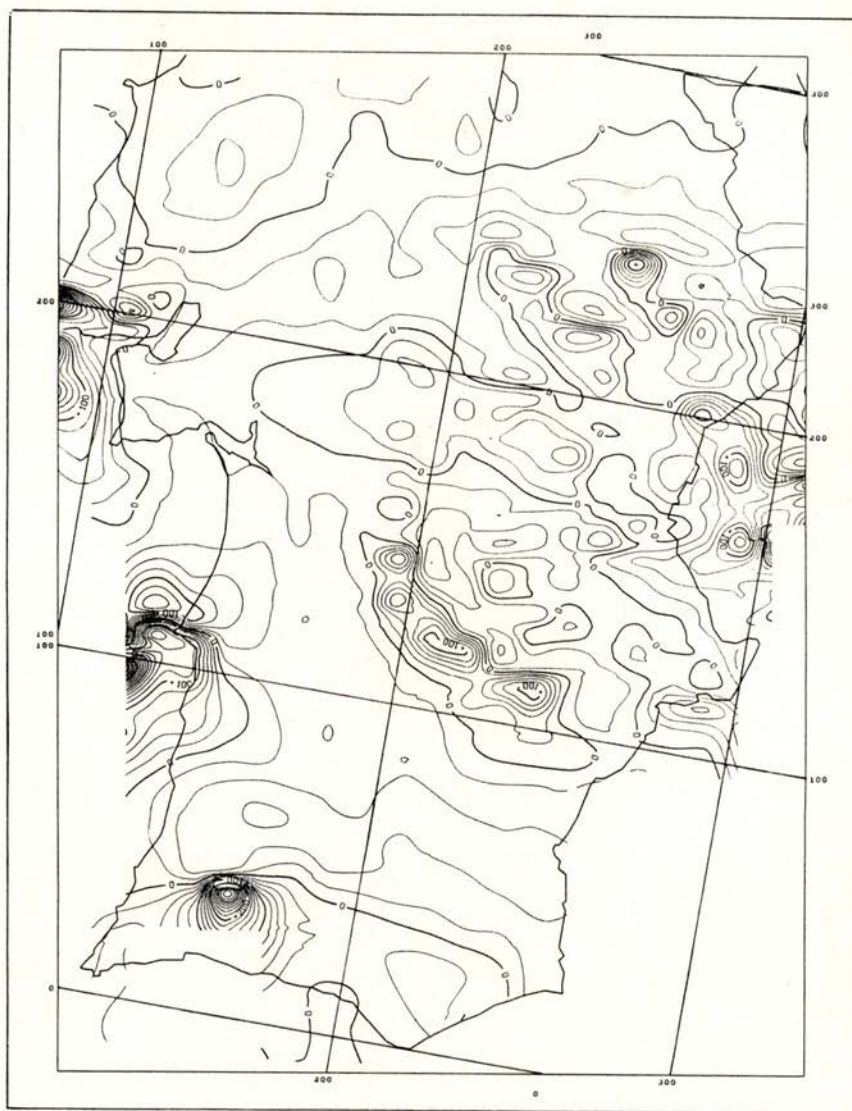


Fig. 12 — Total field anomalies map for southern Portugal (nT).

5 — ACCURACY

The main sources of error have been pointed out already. These include errors due to field measurement, to the uncertainty in the location of the measurement points, and to the time reduction

methods employed. In the last category we must also distinguish between the errors due to the calculation of the Beja mean annual field value and those due to the non-homogeneity of the diurnal variation over the survey area.

The proton precession magnetometer assures a nominal precision of 1 nT. From the smoothing effect (see Fig. 5) we can estimate a maximum of 2 nT for this component of the noise.

Location errors in the horizontal coordinates are small over land (of the order of 50 m) but can be larger over the sea. For seriously anomalous areas (horizontal gradient greater than 20 nT/Km) this can originate an error of 1 or 2 nT over the land. It is surely greater over the sea.

The errors due to the set of the annual mean value for Beja station can be roughly represented by the dispersion of the daily differences (cf. Fig. 2) which is about 4 nT.

The uncertainty in the flight height and in the non-homogeneity of the diurnal variation can only be indirectly estimated by the cross errors between flight and tie-lines.

The final accuracy of the survey can be estimated as ± 10 nT. It must be emphasized that the major part of this uncertainty is a smoothly varying quantity that was distributed along the lines during the reduction process, and so will mainly affect the greater wavelengths presented in the map.

6 — CONCLUSIONS

The aeromagnetic survey of Portugal, the southern pannel of which was here analysed, is intended to be a reliable basis for the design of crustal models.

The authors hope that it will be possible to establish an adequate representation of the main and the crustal magnetic fields for the Portuguese territory after the conclusion of the northern pannel of the survey. The correlation between geology and magnetic behaviour, which is already apparent in the presented maps, demonstrates the importance of this survey as a tool for understanding the deep geology of Portugal.

This work is a result of a great number of individual contributions as the processing of an aeromagnetic survey involves an intimate collaboration between the flight and the observatory operations, the photo identifications and all the other processing techniques. The authors are most indebted to all the personnel of the INMG, in particular to I. Abreu, M. A. Baptista and M. L. Contreiras, and to the geophysical team of the Portuguese accomplishment of the survey.

We wish also to thank Dr. Le Moüel, Director of the Geomagnetism Laboratory of the IPGP, for all the material collaboration that was essential to this work.

REFERENCES

- [1] REINSCH, C. H., «Smoothing by spline functions» *Num. Math.*, **10**, 177/183 (1967).
- [2] AKIMA, A., «A new method of interpolation and smooth curve fitting based on local procedure». *Journ. ACM*, **17**, n.º 4, 589/602 (1970).
- [3] GALDEANO, A., «La cartographie aeromagnetique du sud-ouest de l'Europe et de la region afar. Realisation, methodes de traitement, applications geodinamiques». Thesis presented to the Université de Paris VII (1980).
- [4] RIBEIRO, A. et al., «Introduction a la Geologie Generale du Portugal». *Serviços Geológicos de Portugal* (1979).
- [5] LE MOUËL, J. L., «Sur la distribution des elements magnetiques en France». Thesis presented to the Faculté de Sciences de l'Université de Paris (1969).
- [6] MENDES-VICTOR, L. A., «L'interpretation des mesures gravimétriques magnetiques aux îles du Cap Vert et la théorie de l'expansion des fonds océaniques». Thèse Docteur-ès-Sciences Physiques — Université de Strasbourg, 198 p. (1970).
- [7] BEREZIN, I. S., ZHIDHKOV, Z. P., «Computing Methods». Pergamon Press, London (1965).
- [8] GRANT, F., «A problem in the analysis of geophysical data». *Geophysics*, **XXII**, 309/344 (1957).
- [9] PEDDIE, N., «International Geomagnetic Reference Field: The third generation». *J. Geom. Geol.*, **34**, 309/326 (1982).